Critical Current Oscillations in Strong Ferromagnetic Pi-Junctions

J. W. A. Robinson¹, S. Piano^{1,2}, G. Burnell¹, C. Bell³, and M. G. Blamire¹

- 1. Department of Material Science, University of Cambridge, Pembroke Street, Cambridge CB2 3QZ, UK
 2. Physics Department and CNR-SUPERMAT Laboratory,
 - University of Salerno, Via S. Allende, 84081 Baronissi (SA), Italy
- 3. Kamerlingh Onnes Laboratory, Leiden University, P.O. Box 9504, 2300 RA Leiden, The Netherlands (Dated: 2 June 2006)

We report magnetic and electrical measurements of Nb Josephson junctions with strongly ferromagnetic barriers of Co, Ni and Ni $_{80}$ Fe $_{20}$ (Py). All these materials show multiple oscillations of critical current with barrier thickness implying repeated 0- π phase-transitions in the superconducting order parameter. We show in particular that the Co barrier devices can be accurately modelled using existing clean limit theories and so that, despite the high exchange energy (309 meV), the large I_cR_N value in the π -state means Co barriers are ideally suited to the practical development of superconducting π -shift devices.

PACS numbers: 74.50.+r, 74.25.5V, 74.78.Db, 74.25.Ha.

Although the interplay of superconductivity and ferromagnetism has been the subject of study for many decades [1], theoretical and experimental investigations into the properties of superconductor-ferromagnetic metal (S/F) heterostructures have seen an upsurge in interest in recent years following the experimental observation of 0 to π transitions in the superconducting order parameter in S/F thin films by Ryanzanov et al. [2] and by Kontos et al. [3]. In terms of the Josephson relationship $I_c = I_0 \sin \Delta \phi$, where $\Delta \phi$ is the phase difference between the two S layers, a transition from the 0 to π states implies a change in sign of I_0 from positive to negative. Physically, such a change in sign of I_0 is a consequence of a phase change in the electron pair wave function induced in the F layer by the proximity effect. Experimentally, measurements of I_c are insensitive to the sign of I_0 and hence the absolute I_c is measured; this implies that a change in state from 0 to π will lead to a zero crossing of I_c and a sharp cusp at $I_c = 0$. It is possible to describe the I_c dependence with ferromagnetic thickness (d_F) by the generic expression

$$I_c R_N(d_F) \propto I_c R_N(d_0) \left| \frac{\sin \frac{d_F - d_1}{\xi_2}}{\sin \frac{d_F - d_0}{\xi_1}} \right| \exp \left\{ \frac{d_0 - d_F}{\xi_1} \right\},$$
 (1)

where d_1 is the thickness of the ferromagnet corresponding to the first minimum, and $I_cR_N(d_0)$ is the first experimental value of $I_cR_N(R_N)$ is the normal state resistance). Transitions can be observed as oscillations in the critical temperature (T_c) of S/F multilayers [4, 5, 6, 7] as well as oscillations in the critical current (I_c) of S/F/S junctions with both thickness of the F layer [8, 9, 10] and, for weak ferromagnets whose exchange energy (E_{ex}) is comparable to k_BT_c of the superconductor, with temperature.

The majority of studies of S/F/S structures have concentrated on the use of weak ferromagnets, such as Cu_xNi_{1-x} and Pd_xNi_{1-x} , where the temperature dependence can be observed and where thickness of the ferromagnetic layer over which oscillations in critical temperature or current are observed can be comparatively large. Even where strong ferromagnets have been used, a significant magnetic 'dead' layer corresponding to a loss in total moment [11] is usually ob-

served which complicates the modeling - see table I.

In the dirty limit where the mean free path $L < d_F$ and $L < \hbar \nu_f/E_{ex}$ the two decay lengths, ξ_1 and ξ_2 , take similar values and so multiple oscillations of I_c are not observed. In contrast, in the clean limit where $d_F < L$ and $L > \hbar \nu_f/E_{ex}$ the decay of the envelope determining the modulation amplitude (ξ_1) can be much larger than the oscillation period (ξ_2). Most previous studies, including those using strong ferromagnets, have been performed in the dirty limit; for practical applications, in which large $I_c R_N$ values are required in the π state it is vital to develop high quality clean limit S/F/S devices. A recent report using the ferromagnetic intermetallic Ni₃Al shows I_c oscillations in the clean limit [12], but with a very large magnetic dead layer which is not accounted for in any phenomenological model and which is likely to make practical control of the phase state of the junction difficult.

Co is a proven device material which can be deposited in clean thin film form with accurately controlled thickness; however, it has not been previously applied in S/F/S junctions because the exchange energy was considered to be far too large. In this letter, we report for the first time measurements of junctions containing Co barriers, together with comparative studies of Py and Ni barriers. We show that, unlike Py and Ni and the weak ferromagnets, the Co data fits excellently to clean limit theory. As importantly, the magnetic dead layer in the Co is less then 1 nm allowing precise control of the phase state of Nb/Co/Nb π -junctions.

Nb/Co/Nb, Nb/Py/Nb and Nb/Ni/Nb films were deposited on 10×5 mm silicon (100) substrates coated with a 250 nm thermal oxide. Simultaneously to growing 10×5 mm thin films for patterning, identical 5×5 mm films were deposited for magnetic characterization in a vibrating sample magnetometer (VSM). All of the layers were deposited by d.c. magnetron sputtering at 1.5 Pa and the deposition system was baked out for seven hours and subsequently cooled with liquid nitrogen for at least one hour prior to the deposition, which gave a base pressure better than 5×10^{-6} Pa and an oxygen partial pressure of less than 3×10^{-9} Pa. In a single deposition run, multiple silicon substrates were placed on a rotat-

ing holder which passed in turn under three magnetrons. The thickness of each layer was controlled by setting the angular speed at which the substrates moved under the respective targets and by setting the target power. When depositing Co, Py, and Ni barriers, an acceleration curve was programmed which allowed the angular speed of the substrates to change monotonically as the substrates passed under the relevant targets. The thickness of the Co (d_{Co}) , Py (d_{Py}) and Ni (d_{Ni}) was then dependent on the substrate position, θ , on the rotating holder. With knowledge of the deposition parameters, the rotation was programmed such that $d(d_F)/d\theta$ was a constant. This method of varying d_F guaranteed in all cases that the interfaces between each layer prepared under the same conditions and the only variation was the thickness. To confirm control over the thicknesses we performed X-ray reflectivity of Nb/Co/Nb thin films where the Nb layers had a thickness of 5 nm and the Co barrier thickness was varied from 0.5 nm to 5.0 nm. A series of low angle X-ray scans were made and the thickness of the Co layer $(d_{Co(observed)})$ extracted by fitting the period of the Kiessig fringes using a commercial simulation package (X'Pert Reflectivity). It was found that our expected thicknesses, $d_{Co(expected)}$, was well correlated with $d_{Co(observed)}$ with a mean deviation of 0.18 nm.

To assist in locating the barrier layer in subsequent focused ion beam (FIB) processing, a thin (20 nm) normal metal layer of Cu was embedded in the 250 nm thick Nb electrodes located 50 nm from the ferromagnetic layer (a distance greater then the coherence length of Nb). At 20 nm, the Cu layer is much thinner than the coherence length in Cu and is therefore totally proximitised by the Nb and plays no part in the electrical properties of the junctions. The thicknesses of the F barriers for the Co and Py Josephson junctions was varied from approximately 0.5 nm to 5 nm and the Ni barrier thickness was varied from 1.0 nm to 10 nm. The films were patterned using optical lithography, followed by broad beam Ar ion milling (3 mAcm⁻², 500 V beam) to produce micron scale tracks and contact pads, to allow four-point measurements to be performed. These tracks were then patterned with a Ga⁺ focused ion beam system (Philips/FEI FIB 200) to achieve vertical transport with a device area in the $0.2 - 1 \mu m^2$ range. The FIB technique for processing such junctions has been described in greater detail elsewhere [13]. A micrograph of one of the junctions processed using the FIB for this work is shown as the inset of Fig. 2(a).

To investigate the magnetic properties of our heterostructures we have measured, using a VSM at room temperature, the magnetic moment per unit surface area of the films as a function of F layer thickness (see Fig. 1). Extrapolating the least-squares fit of the data in Fig. 1 gives a nominal magnetic dead layer of ~ 0.75 nm for Co, ~ 0.5 nm for Py and ~ 1.75 nm for Ni. The causes of a magnetic dead layer are often attributed to factors such as lattice mismatch causing elastic deformation, formation of amorphous interfaces and a breakdown in the crystal structure leading to a reduced exchange interaction between neighbouring atoms and hence a reduction in T_{Curie} and E_{ex} [14, 15, 16].

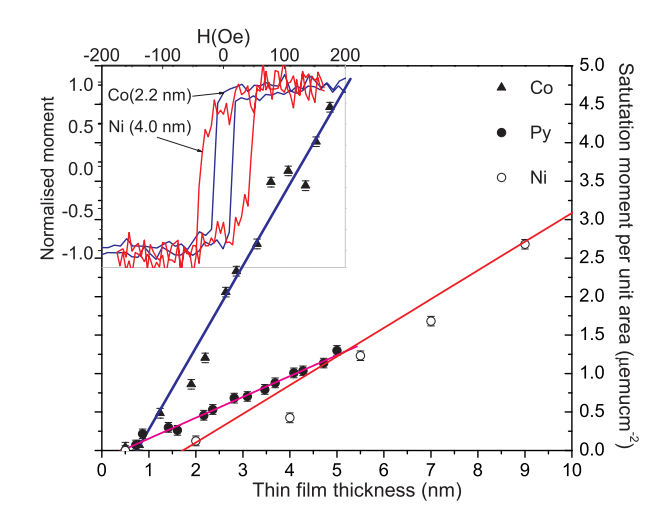


FIG. 1: (Color online) Scaling of the magnetic moment per unit area vs. Co, Py and Ni barrier thickness at room temperature. The best fit lines are least-square fits of the data. Extrapolating the least-squares fit gives a nominal magnetic dead layer of ~ 0.75 nm for Co, ~ 0.5 nm for Py and ~ 1.75 nm for Ni. Inset: hysteresis loops for Co and Ni at room temperature.

Transport measurements were made in a liquid He dip probe. The differential resistance as a function of bias current of the junctions was measured with a standard lock-in technique. The critical current was found from the differential resistance as the point where the differential resistance increases above the value for zero bias current. R_N was measured using a quasi-dc bias current of 3-5 mA, this enabled the nonlinear portion of the I-V curves to be neglected, but was not large enough to drive the Nb electrodes into a normal state. A dV/dI(I) and V(I) plot for a typical Nb-Py-Nb Josephson junction is shown inset of Fig. 2(b). In general, the critical currents of the devices measured for this work ranged from 500 μ A to below the minimum sensitivity of our apparatus (50 nA), while the normal state resistances were in the range 1.0 m Ω to 100 m Ω .

The variation of I_cR_N as a function of Co, Py and Ni thickness at $4.2~\rm K$ is shown in Fig. 2(a-c) respectively. Each point in these figure corresponds to the mean of several junctions with different areas; the vertical error bars are derived from the measured variation in I_cR_N and a small noise contribution due to the current source. From X-ray reflectivity results, as discussed above, we take the error in d_F for all F barriers to be $\approx 0.18~\rm nm$. All of the devices shown in this data set presented Shapiro steps upon the application of microwaves and an I_c modulation with applied field H_A . For the devices where $d_{Co} > 5~\rm nm$, $d_{Py} > 5~\rm nm$, and $d_{Ni} > 13~\rm nm$ some reduction of the differential resistance around $I=0~\rm was$ seen, but did not show a measurable supercurrent at 4.2 K. As expected, I_cR_N for the Co, Py and Ni decreases exponentially and in an oscillatory fashion with d_F .

The Co data was modeled using a equation (1); from the model fit shown in Fig. 2(a) we find that the period of the Co oscillations is ~ 1.91 nm and hence $\xi_2 \sim 0.30$ nm and $\xi_1 \sim$

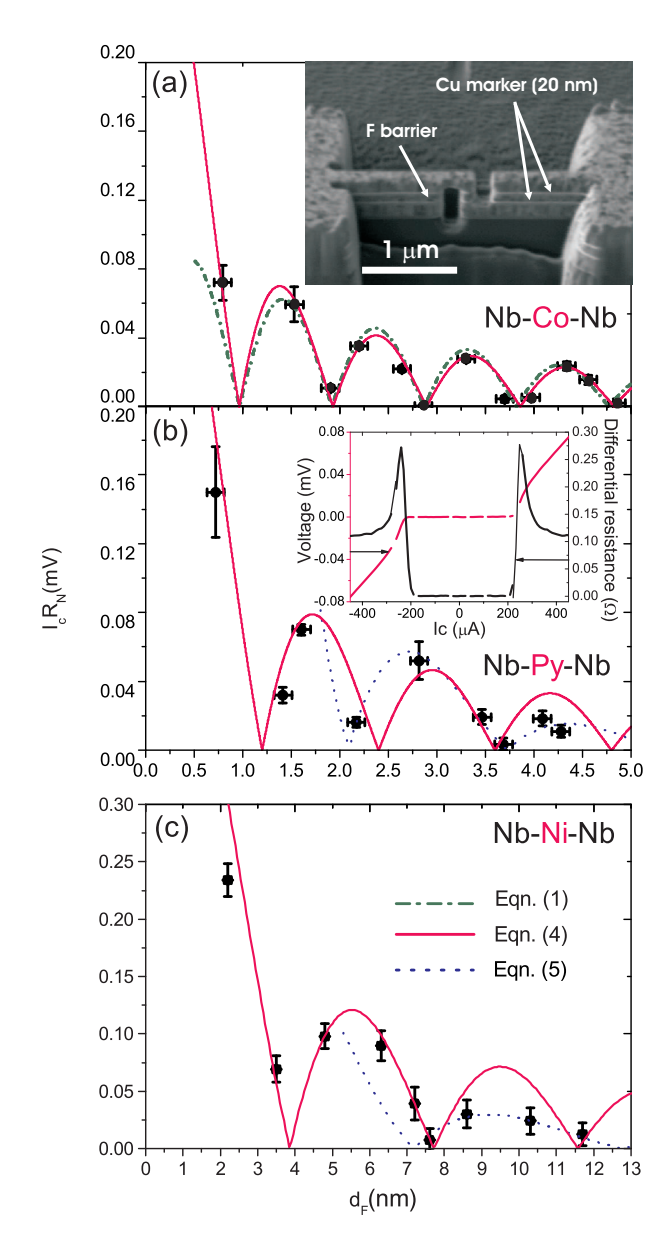


FIG. 2: (Color online) Characteristic voltage, I_cR_N , as a function of Co, Py and Ni thickness at 4.2K. The solid lines are fits to equation (4), the dotted lines are fits to equation (5), and the dashed line is a fit to equation (1) as described in text. Inset (a): An FIB micrograph of a typical Nb-Co-Nb Josephson junction. The two bright lines are the thin Cu layers deposited to help locate the Co barrier and to assist processing the junctions in the FIB system. Inset (b): V(I) and dV/dI(I) plotted for a typical Nb/Py/Nb Josephson junction measured at $4.2~{\rm K}$

3.0 nm. This gives a ξ_2/ξ_1 ratio of ~ 0.11 . A full theoretical treatment involves solving linear Eilenberger equations [17] and yields equation (2)

$$\tanh \frac{L}{\xi_{eff}} = \frac{\xi_{eff}^{-1}}{\xi_0^{-1} + L^{-1} + i\xi_H^{-1}}$$
 (2)

where ξ_{eff} is the effective decay length given by $\xi_{eff}^{-1} = \xi_1^{-1} + i\xi_2^{-1}$, ξ_o is the Ginzburg-Landau coherence length

and ξ_H is a complex coherence length. In the clean limit $1+L\xi_0^{-1}>>\frac{1}{2}\max\{\ln(1+L\xi_0^{-1}),\ln(L\xi_H^{-1})\}$. The solution of equation (2) gives

$$\xi_1^{-1} = \xi_0^{-1} + L^{-1}, \xi_0 = \frac{\nu_F \hbar}{2\pi T_c k_B}, \xi_2 = \xi_H = \frac{\nu_F \hbar}{2E_{cr}},$$
 (3)

and the numerical solution is shown in Fig. (3).

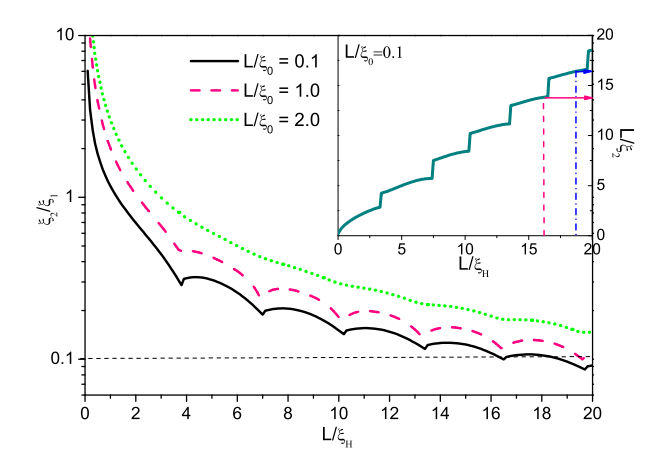


FIG. 3: (Color online) The dependence of ξ_2/ξ_1 with inverse magnetic length, L/ξ_H , calculated for different ratios of L/ξ_0 . Left inset: inverse decay length, $L/\xi_2=f(L/\xi_0)$ for when $L/\xi_0\simeq 0.1$

Following the method of Gusakova and Kupriyanov [17] we find from Fig. (3) that the experimental ratio $\xi_2/\xi_1 \simeq 0.1$ corresponds to two inverse magnetic lengths of $L/\xi_H \sim 16.5$ and $L/\xi_H \sim 18.7$. By assuming $L/\xi_0 \simeq 0.1$ and for the estimated parameters $\xi_1 \sim 3$ nm and $\xi_2 \sim 0.3$ nm we obtained, from the inset in Fig. (3) that for $L/\xi_H \sim 16.5$ and $L/\xi_H \sim 18.7$, $\overline{L} \sim 5$ nm. Inputting these values into equation (3) gives $\nu_F(Co) \simeq 2.8 \times 10^5$ ms⁻¹ which is similar to other reported values of $\nu_F(Co)$ [?] and $E_{ex} \simeq 309$ meV.

To validate the determined mean free path of our Co thin film we have estimated L(Co) in a 50 nm thick Co film by measuring its resistivity as a function of temperature using the Van der Pauw technique. The transport in Co thin films is dominated by free-electron-like behaviour [18] and hence the maximum mean free path is estimated from $L=\hbar k_F/n_e e^2\rho_b$, where n_e is the electron density for Co and is estimated from the ordinary Hall effect to be $5.8\times10^{28}~{\rm cm}^{-3}$ [19] and ρ_b is the residual resistivity. The residual resistance ratio $((\rho_T+\rho_b)/\rho_b)$ was measured to be $\simeq 1.41$ and hence we calculate L_{Co} at $4.2~{\rm K}$ to be 10 nm. This verifies that our estimated $\overline{L}\simeq 5~{\rm nm}$ is a good approximation and this value justifies the assumption of a clean limit fit.

As a comparison we have also modeled the Co oscillations with a simpler theoretical model given by equation (4) [20]

$$I_c R_N \propto \frac{|\sin(2E_{ex}d_F/\hbar\nu_f)|}{2E_{ex}d_F/\hbar\nu_f}.$$
 (4)

As in the case of equation (1) the fitting between the theoretical model and the experimental data is good (see Fig. 2 (a)

ξ_1 (nm)	ξ_2 (nm)	F	$\nu_F (\mathrm{ms}^{-1})$	E_{ex} (meV)	DL(nm)	Ref
1.2	1.6	Ni ₂₀ Fe ₈₀	2.2×10^{5}	95	0.7	[9]
1.4	0.46	$Ni_{20}Fe_{80} \\$	2.2×10^5	201	0.5	*
1.8	2.0	$Pd_{90}Ni_{10} \\$	2.0×10^{5}	35	-	[3]
1.7	1.0	Ni	2.8×10^{5}	200	-	[10]
2.3	0.86	Ni	2.8×10^{5}	107	-	[8]
4.1	1.2	Ni	2.8×10^{5}	80	1.8	*
4.6	0.45	Ni_3Al	1.5×10^{5}	86	5-8	[12]
3.0	0.3	Co	2.8×10^{5}	309	0.8	*

TABLE I: A summary of reported parameters for different material systems. Where DL stands for 'Dead Layer Thickness' and * 'This paper'.

dashed line) and in particular the best fitting has been obtained by using $\nu_F = 2.8 \times 10^5 \text{ ms}^{-1}$ and $E_{ex} = 309 \text{ meV}$.

In contrast, the Py and Ni data cannot be fitted entirely in the clean limit. In the case of Py, equation (4), closely matches the experimental data up to a thickness of ~ 3.6 nm and in the case of Ni the oscillations follow the clean limit theory to ~ 7 nm. Above these values a better fit is obtained using dirty limit formula given by [21]:

$$I_C R_N \propto \mid Re \sum_{\omega_m > 0} \frac{\Delta^2}{\Delta^2 + \omega_m^2} \int_{-1}^1 \frac{\mu}{\sinh(k_\omega d_F/\mu L)} d\mu \mid,$$
 (5)

where Δ is the superconducting order parameter, ω_m is the Matsubara frequency and is given by $\omega_m = \pi T k_B (2m+1)$ where T is the transmission coefficient and m is an integer number. $k_\omega = (1+2\mid \omega_m\mid \tau/\hbar) - 2iE_{ex}\tau/\hbar$ and $\mu = \cos\theta$ where θ is the angle the momentum vector makes relative to the distance normal to the SF interface. L is given by $\nu_f\tau$ and τ is the momentum relaxation time. For equation (4) the only fitting factor, besides the numerical prefactor, was the strength of the exchange interaction $(E_{ex}/\hbar v_f)$. In the case of equation (5) a suitable Fermi velocity, superconducting energy gap and exchange interaction energy had to be chosen. To fit equation (5) to Py and Ni data we used: $\nu_f(Py) = 2.2 \times 10^5$ m/s and $L_{Py} \simeq 2.3$ nm, and $\nu_f(Ni) = 2.8 \times 10^5$ m/s and $L_{Ni} \simeq 7$ nm and $\Delta = 1.3$ meV. These values are consistant with the ones used in equation (4) and elsewhere [8, 9].

From the oscillation period we can estimate the E_{ex} of the Py and Ni barriers - from equation (4) the periodicity is given by $L_{osc} \sim \hbar \nu_f/2E_{ex}$ and hence we can deduce E_{ex} . The exchange energies for Py and Ni were found to be 201 meV and 80 meV respectively. $E_{ex}(Py)$ is approximately double that measured recently in Nb/Py/Nb junctions deposited with epitaxial barriers where E_{ex} was found to be 95 meV [9], but $E_{ex}(Ni)$ is close to other reported values [8].

The fully clean limit behaviour observed with the Co barriers arises most obviously from the use of a pure element, but also from the vertical coherence likely [22] even in noncrys-

talline heterostructures. The high E_{ex} results in a short oscillation period implying a need for Å-level control of layer thickness for practical devices; however Co and Co-alloys form the basis of current spintronic device production, and precision layer control and excellent compatiblity with tunnel barriers [23] have been demonstrated in many industrial processes [24]. Co is therefore an attractive material for qubits and other novel devices.

In summary, we have measured critical current oscillations in Co junctions as a function of Co barrier thickness which indicates that the devices are strongly in the clean limit. This results in a high I_cR_N value in the π state. We also present complementary critical current oscillations through Py and Ni barriers. The oscillations in I_cR_N with d_F are indicative of $0-\pi$ crossovers, but without conducting phase-sensitive measurements the specific phases of the individual junctions cannot be known. The oscillations showed an excellent fit to theoretical models. We have also estimated, from the periodicity of the oscillations, the exchange energies of the Co, Py and Ni barriers to be 309 meV, 201 meV and 80 meV respectively. Results within this paper are summarised in table I alongside results reported elsewhere.

The authors thank M. Yu. Kupriyanov, A. M. Cucolo, and F. Bobba for helpful discussions and N. Stelmashenko for technical assistance. We acknowledge the support of the EPSRC UK and the European Science Foundation π -shift network.

- [1] A. I. Buzdin, Rev. Mod. Phys. 77, 935 (2005).
- [2] V. V. Ryazanov et al., Phys. Rev. Lett. 86, 2427 (2001).
- [3] T. Kontos et al., Phys. Rev. Lett. 89, 137007 (2002).
- [4] J. S. Jiang et al., Phys. Rev. Lett. 74, 314 (1995).
- [5] Th. Mühge et al., Phys. Rev. Lett. 77, 1857 (1996).
- [6] Y. Obi et al., Physica C 317-318, 149 (1999).
- [7] L. Lazar et al., Phys. Rev. B 61, 3711 (2000).
- [8] Y. Blum et al., Phys. Rev. Lett. 89, 187004-1 (2002).
- [9] C.Bell et al., Phys. Rev. B 71, 180501(R) (2005).
- [10] V. Shelukhin et al., cond-mat/0512593 (2006).
- [11] S. Pick et al., St. Commun. 124, 21 (2002).
- [12] F. Born et al., cond-mat/0604277 (2006).
- [13] C. Bell et al., Nanotechnology 14, 630 (2003).
- [14] J. Aarts et al., Phys. Rev. B 56, 2779 (1997).
- [15] R. Zhang and R. F. Willis, Phys. Rev. Lett. 86, 2665 (2001).
- [16] Q. Leng et al., J. Appl. Phys. 87, 6621 (2000).
- [17] D. Yu. Gusakova, M. Yu. Kupriyanov and A. A. Golubov, cond-mat/0605137 (2006).
- [18] B.A. Gurney et al., Phys. Rev. Lett. **71**, 4023 (1996).
- [19] J. Kötzler and W. Gil, Phys. Rev. B 72, 060412(R) (2005).
- [20] A. I. Buzdin, JETP Lett. **35**, 178 (1982).
- [21] F. S. Bergeret et al. Phys. Rev. B 64, 134506 (2001).
- [22] C. W. Leung et al., J. Mag. Mag. Mats. 269 (1), 15 (2004).
- [23] I. I. Oleinik et al., Phys. Rev. B **62**, 3952 (2000)
- [24] C. Kaiser and S. S. P. Parkin, Appl. Phys. Lett., 84, 3582 (2004)